14

Purely irrotational theories of the effect of the viscosity on the decay of waves

14.1 Decay of free gravity waves

It is generally believed that the major effects of viscosity are associated with vorticity. This belief is not always well founded; major effects of viscosity cachap14-sep11-nocup.n be obtained from purely irrotational analysis of flows of viscous fluids. Here we illustrate this point by a comparing irrotational solutions with Lamb's 1932 exact solution of the problem of the decay of free gravity waves. Excellent agreements, even in fluids 10^7 more viscous than water, are achieved for the decay rates $n(k)$ for all wave numbers k excluding a small interval around a critical value k_c where progressive waves change to monotonic decay.

14.1.1 Introduction

Lamb (1932, §348, §349) performed an analysis of the effect of viscosity on free gravity waves. He computed the decay rate by a dissipation method using the irrotational flow only. He also constructed an exact solution for this problem, which satisfies both the normal and shear stress conditions at the interface.

Joseph & Wang (2004) studied Lamb's problem using the theory of viscous potential flow (VPF) and obtained a dispersion relation which gives rise to both the decay rate and wave-velocity. They also used VCVPF to obtain another dispersion relation. Since VCVPF is an irrotational theory the shear stress cannot be made to vanish. However, the shear stress in the energy balance can be eliminated in the mean by the selection of an irrotational pressure which depends on viscosity.

Here we find that the viscous pressure correction gives rise to a higher order irrotational correction to the velocity which is proportional to the viscosity and does not have a boundary layer structure. The corrected velocity depends strongly on viscosity and is not related to vorticity. The corrected irrotational flow gives rise to a dispersion relation which is in splendid agreement with Lamb's exact solution, which has no explicit viscous pressure. The agreement with the exact solution holds for fluids even 10^7 times more viscous than water and for all wave numbers away from the cutoff wave number k_c which marks the place where progressive waves change to monotonic decay. We find that VCVPF gives rise to the same decay rate as in Lamb's exact solution and in his dissipation calculation when $k < k_c$. The exact solution agrees with VPF when $k > k_c$. The effects of vorticity are evident only in a small interval centered on the cutoff wave number. We present a comprehensive comparison for the decay rate and wave-velocity given by Lamb's exact solution and Joseph and Wang's VPF and VCVPF theories.

14.1.2 Irrotational viscous corrections for the potential flow solution

The gravity wave problem is governed by the linearized Navier-Stokes equation and the continuity equation

$$\frac{\partial \mathbf{u}}{\partial t} = -\frac{1}{\rho}\nabla p - g\mathbf{e}_y + \nu\nabla^2\mathbf{u}, \tag{14.1.1}$$

$$\nabla \cdot \mathbf{u} = 0, \tag{14.1.2}$$

subject to the boundary conditions at the free surface ($y \approx 0$)

$$T_{xy} = 0, \quad T_{yy} = 0, \tag{14.1.3}$$

where T_{xy} and T_{yy} are components of the stress tensor and the surface tension is neglected. Surface tension is important at high wavenumbers but, for simplicity, is neglected in the analyses given here. We divide the velocity and pressure field into two parts

$$\mathbf{u} = \mathbf{u}_{\mathrm{p}} + \mathbf{u}_{\mathrm{v}}, \quad p = p_{\mathrm{p}} + p_{\mathrm{v}}, \tag{14.1.4}$$

where the subscript p denotes potential solutions and v denotes viscous corrections. The potential solutions satisfy

$$\mathbf{u}_{\mathrm{p}} = \nabla\phi, \quad \nabla^2\phi = 0, \tag{14.1.5}$$

and

$$\frac{\partial \mathbf{u}_{\mathrm{p}}}{\partial t} = -\frac{1}{\rho}\nabla p_{\mathrm{p}} - g\mathbf{e}_y. \tag{14.1.6}$$

The viscous corrections are governed by

$$\nabla \cdot \mathbf{u}_{\mathrm{v}} = 0, \tag{14.1.7}$$

$$\frac{\partial \mathbf{u}_{\mathrm{v}}}{\partial t} = -\frac{1}{\rho}\nabla p_{\mathrm{v}} + \nu\nabla^2\mathbf{u}_{\mathrm{v}}. \tag{14.1.8}$$

We take the divergence of (14.1.8) and obtain

$$\nabla^2 p_{\mathrm{v}} = 0, \tag{14.1.9}$$

which shows that the pressure correction must be harmonic. Next we introduce a stream function ψ so that (14.1.7) is satisfied identically:

$$u_{\mathrm{v}} = -\frac{\partial\psi}{\partial y}, \quad v_{\mathrm{v}} = \frac{\partial\psi}{\partial x}. \tag{14.1.10}$$

We eliminate p_{v} from (14.1.8) by cross differentiation and obtain following equation for the stream function

$$\frac{\partial}{\partial t}\nabla^2\psi = \nu\nabla^4\psi. \tag{14.1.11}$$

To determine the normal modes which are periodic in respect of x with a prescribed wave-length $\lambda = 2\pi/k$, we assume that

$$\psi = B\mathrm{e}^{nt+\imath kx}\mathrm{e}^{my}, \tag{14.1.12}$$

where m is to be determined from (14.1.11). Inserting (14.1.12) into (14.1.11), we obtain

$$(m^2 - k^2)\left[n - \nu(m^2 - k^2)\right] = 0. \tag{14.1.13}$$

The root $m^2 = k^2$ gives rise to irrotational flow; the root $m^2 = k^2 + n/\nu$ leads to the rotational component of the flow. The rotational component cannot give rise to a harmonic pressure satisfying (14.1.9) because

$$\nabla^2\mathrm{e}^{nt+\mathrm{i}kx}\mathrm{e}^{my} = (m^2 - k^2)\mathrm{e}^{nt+\mathrm{i}kx}\mathrm{e}^{my} \tag{14.1.14}$$

does not vanish if $m^2 \neq k^2$. Thus, the governing equation for the rotational part of the flow can be written as

$$\frac{\partial\psi}{\partial t} = \nu\nabla^2\psi. \tag{14.1.15}$$

This is the equation used by Lamb (1932) for the rotational part of his exact solution.

The effect of viscosity on the decay of a free gravity wave can be approximated by a purely irrotational theory in which the explicit appearance of the irrotational shear stress in the mechanical energy equation is eliminated by a viscous contribution p_{v} to the irrotational pressure. In this theory $\mathbf{u}{=}\nabla\phi$ and a stream function, which is associated with vorticity, is not introduced. The kinetic energy, potential energy and dissipation of the flow can be computed using the potential flow solution

$$\phi = A\mathrm{e}^{nt+ky+\mathrm{i}kx}. \tag{14.1.16}$$

We insert the potential flow solution into the mechanical energy equation (12.5.14)

$$\int_{S_{\mathrm{f}}} u_{\mathrm{n}}\left[\rho\left(\frac{\partial\phi}{\partial t} + \frac{|\nabla\phi|^2}{2} + g\eta\right) + 2\mu\frac{\partial^2\phi}{\partial n^2} + \gamma\nabla_{\mathrm{II}}\cdot\mathbf{n}\right]\mathrm{d}S_{\mathrm{f}} = -\int_{S_{\mathrm{f}}}\tau_{\mathrm{s}}u_{\mathrm{s}}\mathrm{d}S_{\mathrm{f}}, \tag{14.1.17}$$

where η is the elevation of the surface and $\mathbf{D}$ is the rate of strain tensor. The pressure correction $p_{\rm v}$ satisfies

$$\int_0^\lambda v(-p_{\rm v})\mathrm{d}x = \int_0^\lambda u\tau_{xy}\mathrm{d}x. \tag{14.1.18}$$

But in our problem here, there is no explicit viscous pressure function in the exact solution [see (14.1.23) and (14.1.24)]. It turns out that the pressure correction defined here in the purely irrotational flow is related to quantities in the exact solution in a complicated way which requires further analysis [see (14.1.30)].

Joseph & Wang (2004) solved for the harmonic pressure correction from (14.1.9), then determined the constant in the expression of $p_{\rm v}$ using (14.1.18), and obtained

$$p_{\rm v} = -2\mu k^2 A\mathrm{e}^{nt+ky+\mathrm{i}kx}. \tag{14.1.19}$$

The velocity correction associated with this pressure correction can be obtained from (14.1.8). We seek normal modes solution $\mathbf{u}_{\rm v} \sim \mathrm{e}^{nt+ky+\imath kx}$ and equation (14.1.8) becomes

$$\rho n\mathbf{u}_{\rm v} = -\nabla p_{\rm v}. \tag{14.1.20}$$

Hence, $\mathrm{curl}(\mathbf{u}_{\rm v}) = 0$ and $\mathbf{u}_{\rm v}$ is irrotational. After assuming $\mathbf{u}_{\rm v} = \nabla\phi_1$ and $\phi_1 = A_1\mathrm{e}^{nt+ky+\mathrm{i}kx}$, we obtain

$$\rho n\phi_1 = -p_{\rm v} \quad \Rightarrow \quad \phi_1 = \frac{2\mu k^2}{\rho n}A\mathrm{e}^{nt+ky+\mathrm{i}kx}. \tag{14.1.21}$$

Given ϕ_1, the correction η_1 of η can be computed from the equation $n\eta = \partial\phi_1/\partial y$.

This calculation shows that the velocity $\mathbf{u}_{\rm v}$ associated with the pressure correction is irrotational. The pressure correction (14.1.19) is proportional to μ and it induces a correction ϕ_1 given by (14.1.21), which is also proportional to μ. The shear stress computed from $\mathbf{u}_{\rm v} = \nabla\phi_1$ is then proportional to μ^2. To balance this non-physical shear stress, one can add a pressure correction proportional to μ^2, which will in turn induce a correction for the velocity potential proportional to μ^2. One can continue to build higher order corrections and they will all be irrotational. The final velocity potential has the following form

$$\phi = (A + A_1 + A_2 + \cdots)\mathrm{e}^{nt+ky+\mathrm{i}kx}, \tag{14.1.22}$$

where $A_1 \sim \mu$, $A_2 \sim \mu^2$... Thus the VCVPF theory is an approximation to the exact solution based on solely potential flow solutions, but the normal stress condition and n are not corrected.

Prosperetti (1976) considered viscous effects on standing free gravity waves using the same governing equations (14.1.7) and (14.1.8) for the viscous correction terms. If we adapt our VCPVF method to treat standing waves represented by the potential $\phi = k^{-1}(\mathrm{d}a/\mathrm{d}t)\mathrm{e}^{ky}\cos kx$, we can obtain $-p_{\rm v} = 2\mu k(\mathrm{d}a/\mathrm{d}t)\mathrm{e}^{ky}\cos kx$, which is exactly the same pressure correction obtained by Prosperetti (1976) using a different method.

14.1.3 Relation between the pressure correction and Lamb's exact solution

It has been conjectured and is widely believed (Moore 1963; Harper and Moore 1968; Joseph and Wang 2004) that a viscous pressure correction arises in the vortical boundary layer at the free surface which is neglected in the irrotational analysis. However, no viscous pressure correction arises in Lamb's exact solution. His solution is given by a potential ϕ and a stream function ψ:

$$u = \frac{\partial\phi}{\partial x} - \frac{\partial\psi}{\partial y}, \quad v = \frac{\partial\phi}{\partial y} + \frac{\partial\psi}{\partial x}, \quad \frac{p}{\rho} = -\frac{\partial\phi}{\partial t} - gy, \tag{14.1.23}$$

satisfying

$$\nabla^2\phi = 0, \quad \partial\psi/\partial t = \nu\nabla^2\psi. \tag{14.1.24}$$

The stream function gives rise to the rotational part of the flow. No pressure term enters into the stream function equation, as we have shown in the previous section that the only harmonic pressure for the rotational part is zero. The pressure p comes from Bernoulli's equation in (14.1.23) and no explicit viscous pressure exists, though p depends on the viscosity through the velocity potential. Lamb shows that (14.1.24) can be solved with normal modes

$$\phi = A\mathrm{e}^{ky}\mathrm{e}^{\mathrm{i}kx+nt}, \quad \psi = C\mathrm{e}^{my}\mathrm{e}^{\mathrm{i}kx+nt}, \quad m^2 = k^2 + n/\nu, \tag{14.1.25}$$

where A and C are constants.

k	$p_{\rm v}/\rho$	term1	term2	term 3	term 4
0.01	-2.063×10^{-6}	$-1.325\times10^{-9}+$ $\imath 2.01\times10^{-4}$	$-2.063\times10^{-6}-$ $\imath 2.01\times10^{-4}$	-1.325×10^{-9}	$5.300\times10^{-9}+$ $\imath 5.300\times10^{-9}$
0.1	-2.057×10^{-4}	$-7.441\times10^{-7}+$ $\imath 0.00358$	$-2.071\times10^{-4}-$ $\imath 0.00358$	-7.461×10^{-7}	$2.980\times10^{-6}+$ $\imath 2.980\times10^{-6}$
1	-0.02022	$-4.207\times10^{-4}+$ $\imath 0.06272$	$-0.02106-$ $\imath 0.06440$	-4.186×10^{-4}	$0.001679+$ $\imath 0.001679$
10	-1.881	$-0.3131+\imath 0.6303$	$-2.423-\imath 1.513$	-0.1829	$1.038+\imath 0.8830$

Table 14.1. *The value of each term in (14.1.30) normalized by A^E for SO10000 oil at different wave numbers; term1 = $\partial\left(\phi^J-\phi^E\right)/\partial t$, term2 = $g(\eta^J-\eta^E)$, term3 =$2\nu\partial^2\left(\phi^J-\phi^E\right)/\partial y^2$, and term4 = $2\nu\partial^2\psi^E/\partial x\partial y$.*

It is therefore of interest to derive the connection between the viscous pressure correction $p_{\rm v}$ in our VCVPF theory and Lamb's exact solution; superscript E represents Lamb's exact solution and J represent Joseph and Wang's VCVPF theory. The irrotational pressure in the two solutions are

$$p^E=-\rho\frac{\partial\phi^E}{\partial t}-\rho g\eta^E,\quad p_{\rm i}^J=-\rho\frac{\partial\phi^J}{\partial t}-\rho g\eta^J. \tag{14.1.26}$$

The elevation η is obtained from the kinematic condition at $y\approx 0$

$$\frac{\partial\eta}{\partial t}^E=\frac{\partial\phi^E}{\partial y}+\frac{\partial\psi^E}{\partial x},\quad \frac{\partial\eta}{\partial t}^J=\frac{\partial\phi^J}{\partial y}. \tag{14.1.27}$$

The normal stress balance for the two solutions is

$$T_{yy}^E=-p^E+2\mu\frac{\partial^2\phi^E}{\partial^2 y}+2\mu\frac{\partial^2\psi^E}{\partial x\partial y}=0, \tag{14.1.28}$$

$$T_{yy}^J=-p_{\rm i}^J-p_{\rm v}+2\mu\frac{\partial^2\phi^J}{\partial^2 y}=0. \tag{14.1.29}$$

Therefore $T_{yy}^E-T_{yy}^J=0$ and we can obtain

$$\frac{p_{\rm v}}{\rho}=\frac{\partial\left(\phi^J-\phi^E\right)}{\partial t}+g(\eta^J-\eta^E)+2\nu\frac{\partial^2\left(\phi^J-\phi^E\right)}{\partial y^2}-2\nu\frac{\partial^2\psi^E}{\partial x\partial y}. \tag{14.1.30}$$

The amplitude A for the potential is different in Lamb's exact solution and in VCPVF:

$$\phi^E=A^E{\rm e}^{nt+ky+{\rm i}kx},\quad \phi^J=A^J{\rm e}^{nt+ky+{\rm i}kx},\quad A^E\neq A^J. \tag{14.1.31}$$

To make the two solutions comparable, we compute the relation between A^E and A^J by equating the dissipation evaluated using Lamb's exact solution and evaluated using VCVPF. In Table 14.1 we list the values of each term in (14.1.30) normalized by A^E. It seems that the term $g(\eta^J-\eta^E)$ gives the most important contribution to p_v, but the other terms are not negligible.

14.1.4 Comparison of the decay rate and wave-velocity given by the exact solution, VPF and VCVPF

When the surface tension is ignored, Lamb's exact solution gives rise to the following dispersion relation:

$$n^2+4\nu k^2n+4\nu^2k^4+gk=4\nu^2k^3\sqrt{k^2+n/\nu}. \tag{14.1.32}$$

Lamb considered the solution of (14.1.32) in the limits of small k and large k. When $k\ll k_c=({\rm g}/\nu^2)^{1/3}$, he obtained approximately

$$n=-2\nu k^2\pm{\rm i}k\sqrt{g/k}, \tag{14.1.33}$$

which gives rise to the decay rate $-2\nu k^2$, in agreement with the dissipation result, and the wave-velocity $\sqrt{g/k}$, which is the same as the wave-velocity for inviscid potential flow. When $k\gg k_c=({\rm g}/\nu^2)^{1/3}$, Lamb noted that the two roots of (14.1.32) are both real. One of them is

$$n_1=-\frac{g}{2\nu k}, \tag{14.1.34}$$

and the other one is

$$n_2 = -0.91\nu k^2. \tag{14.1.35}$$

Lamb pointed out n_1 is the more important root because the motion corresponding to n_2 dies out very rapidly.

14.1.4.1 VPF results

Joseph & Wang (2004) treated this problem using VPF and obtained the following dispersion relation

$$n^2 + 2\nu k^2 n + gk = 0. \tag{14.1.36}$$

When $k < k_c = (\mathrm{g}/\nu^2)^{1/3}$, the solution of (14.1.36) is

$$n = -\nu k^2 \pm \mathrm{i}k\sqrt{g/k - \nu^2 k^2}. \tag{14.1.37}$$

We note that the decay rate $-\nu k^2$ is half of that in (14.1.33) and the wave-velocity $\sqrt{g/k - \nu^2 k^2}$ is slower than the inviscid wave-velocity. When $k > k_c = (\mathrm{g}/\nu^2)^{1/3}$, the two roots of (14.1.36) are both real and they are

$$n = -\nu k^2 \pm \sqrt{\nu^2 k^4 - gk}. \tag{14.1.38}$$

If $k \gg k_c = (\mathrm{g}/\nu^2)^{1/3}$, the above two roots are approximately

$$n_1 = -\frac{g}{2\nu k}, \tag{14.1.39}$$

and

$$n_2 = -2\nu k^2 + \frac{g}{2\nu k}. \tag{14.1.40}$$

We note that (14.1.39) is the same as (14.1.34), and the magnitude of (14.1.40) is approximately twice of (14.1.35).

14.1.4.2 VCVPF results

Joseph & Wang (2004) computed a pressure correction and added it to the normal stress balance to obtain

$$n^2 + 4\nu k^2 n + gk = 0, \tag{14.1.41}$$

which is the dispersion relation for VCVPF theory. When $k < k_c' = (\mathrm{g}/4\nu^2)^{1/3}$, the solution of (14.1.41) is

$$n = -2\nu k^2 \pm \mathrm{i}k\sqrt{g/k - 4\nu^2 k^2}. \tag{14.1.42}$$

We note that the decay rate $-2\nu k^2$ is the same as in (14.1.33) and the wave-velocity $\sqrt{g/k - 4\nu^2 k^2}$ is slower than the inviscid wave-velocity. When $k > k_c' = (\mathrm{g}/4\nu^2)^{1/3}$, the two roots of (14.1.41) are both real and they are

$$n = -2\nu k^2 \pm \sqrt{4\nu^2 k^4 - gk}. \tag{14.1.43}$$

If $k \gg k_c' = (\mathrm{g}/4\nu^2)^{1/3}$, the above two roots are approximately

$$n_1 = -\frac{g}{4\nu k}, \tag{14.1.44}$$

and

$$n_2 = -4\nu k^2 + \frac{g}{4\nu k}. \tag{14.1.45}$$

We note that (14.1.44) is half of (14.1.34), and the magnitude of (14.1.45) is approximately four times of (14.1.35).

Fluid	water	glycerin	SO10000	–
$\nu(\mathrm{m}^2/\mathrm{s})$	10^{-6}	6.21×10^{-4}	1.03×10^{-2}	10
$k_c(1/\mathrm{m})$	21399.7	294.1	45.2	0.461

Table 14.2. *The values for the cutoff wave number k_c for water, glycerin, SO10000 oil and the liquid with ν= 10 m^2/s. k_c decreases as the viscosity increases.*

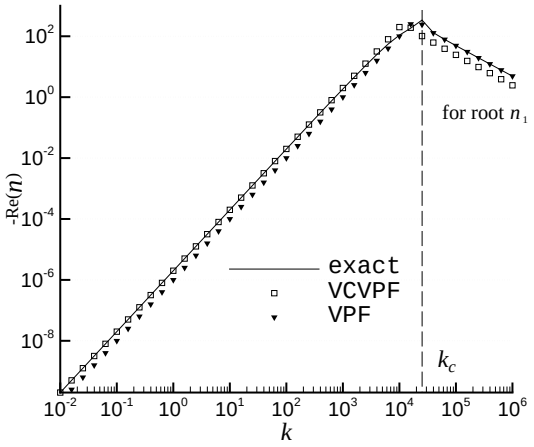

Fig. 14.1. Decay rate $-\mathrm{Re}(n)$ vs. wave number k for water, $\nu = 10^{-6}$ m^2/s. $\mathrm{Re}(n)$ is computed for the exact solution from (14.1.32), for VPF from (14.1.36) and for VCVPF from (14.1.41). When $k < k_c$, the decay rate $-2\nu k^2$ for VCVPF is in good agreement with the exact solution, whereas the decay rate $-\nu k^2$ for VPF is only half of the exact solution. When $k > k_c$, n has two real solutions in each theory. In this figure, we plot the decay rate n_1 corresponding to (14.1.34), (14.1.39) and (14.1.44). The exact solution can be approximated by $-g/(2\nu k)$; the decay rate $-g/(2\nu k)$ for VPF is in agreement with the exact solution, whereas the decay rate $-g/(4\nu k)$ for VCVPF is only half of the exact solution.

14.1.4.3 Comparison of the exact and purely irrotational solutions

We compute the solution of (14.1.32) and compare the real and imaginary part of n with those obtained by solving (14.1.36) and (14.1.41). Water, glycerin and SO10000 oil, for which the kinematic viscosity is 10^{-6}, 6.21×10^{-4}, and 1.03×10^{-2} m^2/s, respectively, are chosen as examples. Figures 14.1 and 14.2 show the decay rate $-\mathrm{Re}(n)$ for water; the root n_1 when $k > k_c$ is shown in figure 14.1 and the root n_2 in figure 14.2. The imaginary part of n, i.e. the wave-velocity multiplied by k, is plotted in figure 14.3 for water. For glycerin and SO10000 oil (figures 14.4 and 14.5), we only plot the decay rate corresponding to the more important root n_1; the plots for the root n_2 and the wave-velocity are omitted. Figure 14.6 shows the decay rate corresponding to the root n_1 for $\nu = 10$ m^2/s, which is 1000 times more viscous than SO10000 oil; the comparison between the exact solution and VPF, VCVPF is still excellent. The cutoff wave number $k_c = (g/\nu^2)^{1/3}$ decreases as the viscosity increases. In Table 14.2 we list the values of k_c for water, glycerin, SO10000 oil and the liquid with ν= 10 m^2/s. In practice waves associated with different wave numbers may exist simultaneously. For very viscous fluids, k_c is small and the majority of the wave numbers are above k_c, therefore the motion of monotonic decay dominates; for less viscous fluids, the motion of progressive waves may dominate.

14.1.5 Why does the exact solution agree with VCVPF when $k < k_c$ and with VPF when $k > k_c$?

Our VCVPF solution and Lamb's dissipation calculation are based on the assumption that the energy equation (14.1.17) for the exact solution is well approximated by an irrotational solution. To verify this, we computed and compared the rates of change of the kinetic energy, the potential energy and dissipation terms in (14.1.17) for Lamb's exact solution and for the purely irrotational part of his solution. The agreement is excellent when $k < k_c$. This shows that the vorticity may be neglected in the computation of terms in the energy balance when $k < k_c$, and is consistent with results given in §14.1.4 which demonstrate that the decay rates from VCVPF and the dissipation calculation agree with the exact solution when k is small. The agreement is poor for k in

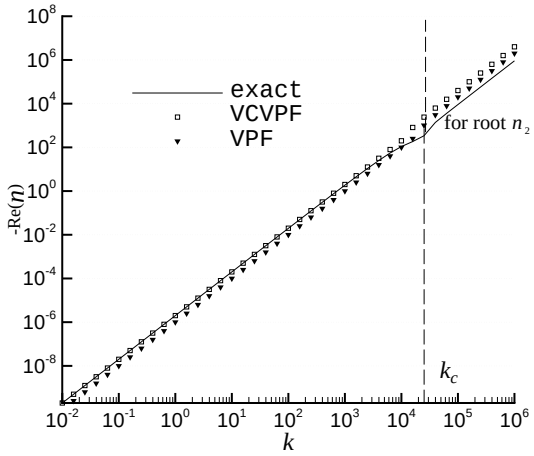

Fig. 14.2. Decay rate $-\mathrm{Re}(n)$ vs. wave number k for water, $\nu = 10^{-6}$ m^2/s. $\mathrm{Re}(n)$ is computed for the exact solution from (14.1.32), for VPF from (14.1.36) and for VCVPF from (14.1.41). When $k > k_c$, n has two real solutions in each theory. In this figure, we plot the decay rate n_2 corresponding to (14.1.35), (14.1.40) and (14.1.45). The decay rate for the exact solution can be approximated by $-0.91\nu k^2$; the decay rate $\approx -2\nu k^2$ for VPF is closer to the exact solution than the decay rate $\approx -4\nu k^2$ for VCVPF.

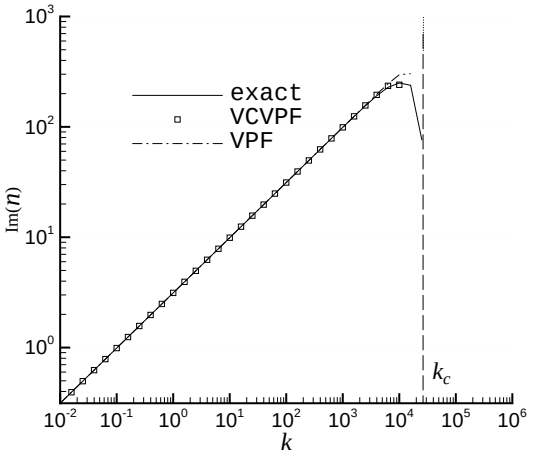

Fig. 14.3. $\mathrm{Im}(n)$, i.e. the wave-velocity multiplied by k, vs. wave number k for water, ν=10^{-6}m^2/s. $\mathrm{Im}(n)$ is computed for the exact solution from (14.1.32), for VPF from (14.1.36) and for VCVPF from (14.1.41). When $k < k_c$, the three theories give almost the same wave-velocity. When $k > k_c$, all the three theories give zero imaginary part of n.

the vicinity of k_c, therefore the decay rates from VCVPF deviate from the exact solution near k_c as shown in figures 14.1-14.6.

When k is much larger than k_c, the energy equation is not well approximated by the irrotational part of the exact solution. However, this result does not mean that the vorticity is important. Lamb pointed out $m \approx k$ when k is large, which is confirmed in our calculation. It follows that the vorticity of the exact solution is

$$\nabla^2\psi = \left(m^2 - k^2\right) C\mathrm{e}^{my+\mathrm{i}kx+nt} \approx 0; \tag{14.1.46}$$

the vorticity is negligible when k is large. The result that the wave is nearly irrotational for large k was also pointed out by Tait (1890). Consequently, the decay rate $-g/(2\nu k)$ from VPF is in good agreement with the exact solution and no pressure correction is needed.

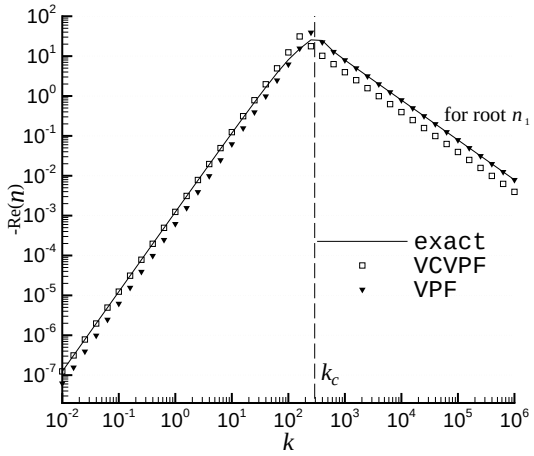

Fig. 14.4. Decay rate $-\mathrm{Re}(n)$ vs. wave number k for glycerin, $\nu = 6.21 \times 10^{-4}\mathrm{m}^2/\mathrm{s}$. $\mathrm{Re}(n)$ is computed for the exact solution from (14.1.32), for VPF from (14.1.36) and for VCVPF from (14.1.41). When $k < k_c$, the decay rate $-2\nu k^2$ for VCVPF is in good agreement with the exact solution, whereas the decay rate $-\nu k^2$ for VPF is only half of the exact solution. When $k > k_c$, n has two real solutions in each theory. In this figure, we plot the decay rate n_1 corresponding to (14.1.34), (14.1.39) and (14.1.44). The decay rate for the exact solution can be approximated by $-g/(2\nu k)$; the decay rate $-g/(2\nu k)$ for VPF is in agreement with the exact solution, whereas the decay rate $-g/(4\nu k)$ for VCVPF is only half of the exact solution.

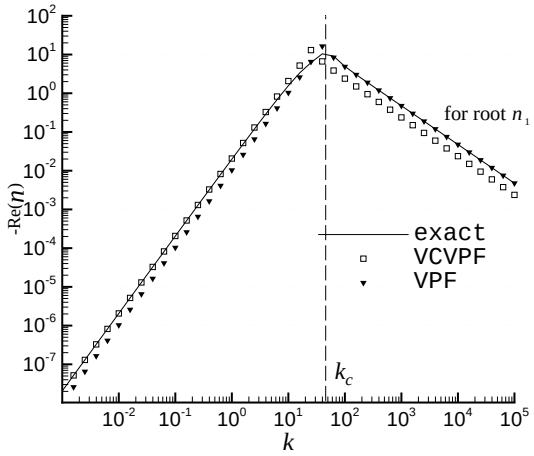

Fig. 14.5. Decay rate $-\mathrm{Re}(n)$ vs. wave number k for SO10000 oil, $\nu = 1.03 \times 10^{-2}\ \mathrm{m}^2/\mathrm{s}$. $\mathrm{Re}(n)$ is computed for the exact solution from (14.1.32), for VPF from (14.1.36) and for VCVPF from (14.1.41). When $k < k_c$, the decay rate $-2\nu k^2$ for VCVPF is in good agreement with the exact solution, whereas the decay rate $-\nu k^2$ for VPF is only half of the exact solution. When $k > k_c$, n has two real solutions in each theory. In this figure, we plot the decay rate n_1 corresponding to (14.1.34), (14.1.39) and (14.1.44). The decay rate for the exact solution can be approximated by $-g/(2\nu k)$; the decay rate $-g/(2\nu k)$ for VPF is in agreement with the exact solution, whereas the decay rate $-g/(4\nu k)$ for VCVPF is only half of the exact solution.

14.1.6 Conclusion and discussion

The problem of decay of free gravity waves due to viscosity was analyzed using two different theories of viscous potential flow, VPF and VCVPF. The pressure correction leads to a hierarchy of potential flows in powers of viscosity. These higher order contributions vanish more rapidly than the principal correction which is proportional to μ. The higher order corrections do not have a boundary layer structure and may not have a physical significance.

The irrotational theory is in splendid agreement with Lamb's exact solution for all wave numbers k except for those in a small interval around k_c where progressive waves change to monotonic decay. VCVPF agrees with Lamb's solution when $k < k_c$ (progressive waves) and VPF agrees with Lamb's exact solution when $k > k_c$ (monotonic decay). The cutoff wave number $k_c = (g/\nu^2)^{1/3}$ decreases as the viscosity increases. In practice

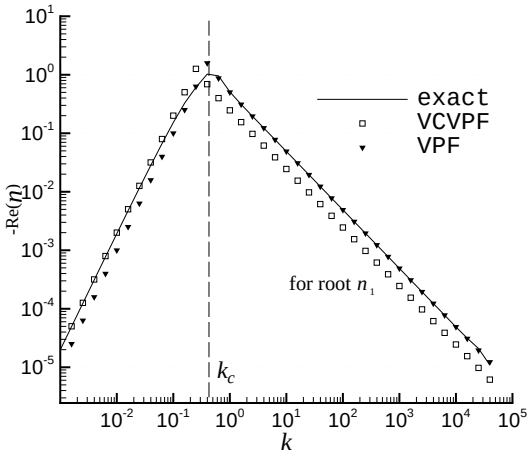

Fig. 14.6. Decay rate $-\mathrm{Re}(n)$ vs. wave number k for ν=10 m^2/s. $\mathrm{Re}(n)$ is computed for the exact solution from (14.1.32), for VPF from (14.1.36) and for VCVPF from (14.1.41). When $k < k_c$, the decay rate $-2\nu k^2$ for VCVPF is in good agreement with the exact solution, whereas the decay rate $-\nu k^2$ for VPF is only half of the exact solution. When $k > k_c$, n has two real solutions in each theory. In this figure, we plot the decay rate n_1 corresponding to (14.1.34), (14.1.39) and (14.1.44). The decay rate for the exact solution can be approximated by $-g/(2\nu k)$; the decay rate $-g/(2\nu k)$ for VPF is in agreement with the exact solution, whereas the decay rate $-g/(4\nu k)$ for VCVPF is only half of the exact solution.

waves associated with different wave numbers may exist simultaneously. For very viscous fluids, k_c is small and the majority of the wave numbers are above k_c, therefore the motion of monotonic decay dominates; for less viscous fluids, the motion of progressive waves may dominate.

There is a boundary layer of vorticity associated with the back and forth motion of the progressive waves. The confined vorticity layer has almost no effect on the solution except for k near k_c. There is no explicit pressure correction in the exact solution. The vortical part of the exact solution does not generate a pressure correction; the pressure depends on the viscosity through the velocity potential and the surface elevation; it is related to the potential and vortical parts of the exact solution in a complicated way. The vortical part is not dominant and the pressure correction is not primarily associated with a boundary layer [see (14.1.30) and Table 14.1].

The analysis of capillary instability of liquid in gas (Wang, Joseph & Funada 2005) is very much like the analysis of the decay of free gravity waves. The purely potential flow analysis is in splendid agreement with Tomotika's (1935) exact solution which has no explicit dependence on viscous pressure. In the case of capillary instability, the best result is based on VCVPF because the short waves which give rise to a sluggish decay in Lamb's problem are stabilized by surface tension.

14.1.7 Quasipotential approximation – vorticity layers

A tractable theory for weakly damped, nonlinear Stokes waves was formulated by Ruvinsky and Freidman (1985a, b; 1987). This theory has come to known as the quasi-potential approximation. The approximation is based on a Helmholtz decomposition

$$\boldsymbol{u} = \nabla\phi + \boldsymbol{v} \tag{14.1.47}$$

where $\boldsymbol{v}$ is the rotational part. They apply a boundary-layer approximation to $\boldsymbol{v}$ and obtain the following system of coupled equations

$$\nabla^2\phi = 0, \quad \frac{\partial\phi}{\partial z} \to 0, \text{ as } z \to \infty \tag{14.1.48}$$

and, on $z = \eta$

$$\frac{\partial\phi}{\partial t} + \frac{1}{2}\left|\nabla\phi\right|^2 + g\eta - \frac{\gamma}{\rho}\kappa + 2\nu\frac{\partial^2\phi}{\partial z^2} = 0, \tag{14.1.49}$$

$$\frac{\partial\eta}{\partial t} + \frac{\partial\eta}{\partial x}\frac{\partial\phi}{\partial x} = \frac{\partial\phi}{\partial z} + v_z \tag{14.1.50}$$

where $\kappa = \left(\partial^2\eta/\partial x^2\right) / \left(1 + (\partial\eta/\partial x)^2\right)^{3/2}$ and v_z is the vertical component of the rotational velocity satisfying

$$\frac{\partial v_z}{\partial t} = 2\nu \frac{\partial^3 \phi}{\partial x^2 \partial z}. \tag{14.1.51}$$

These are three equations in ϕ, η and v_z. The derivation of these is such that v_z is assumed small. This is one reason why the quasipotential approximation is said to model weak effects of viscosity.

Spivak *et al.* 2002 applied the quasi-potential methodology, for a slightly viscous fluid and small surface elasticity, to numerically compute typical free surface profiles induced by a moving pressure distribution under the combined effects of gravity, viscosity, surface tension and film elasticity.

Ruvinsky, Feldstein and Freidman 1991 carried out simulations of ripple excitation by steep gravity capillary waves. They note that when describing the capillary-gravity excitation phenomenon, dissipative processes must be taken into account. "In an exact formulation, this problem has not yet been solved even with a computer." To solve their problem they used the quasi-potential methodology.

Longuet-Higgins 1992 gave a simplified derivation of the quasi-potential methodology in an application to the theory of weakly damped Stokes waves. He gave a simpler form of the equations by applying the boundary conditions on a slightly displaced surface.

Are the principal effects of viscosity associated with vorticity or are they purely irrotational? In his 1992 paper Longuet-Higgins says that "... Lamb 1932 ... showed that for most wavelengths of interest the effects of viscosity on linear, deep-water waves are confined to a thin vortex layer near the free surface, of thickness $D_0 = (2\nu/\gamma)^{1/2}$ (where ν denotes the kinematic viscosity and σ the radian frequency). When $kD_0 \ll 1$ (k the wavenumber) we may say that the waves are weakly damped."

The foregoing statement by Longuet-Higgins is not correct. The effects of viscosity are not confined to a thin vortex layer; the main effects of viscosity on the decay of waves are irrotational. Typically the effects of viscosity arising from the boundary layer at a gas-liquid surface are small because the rates of strain in these layers are no larger than in the irrotational flow and the layer thickness is small. In a later work, Longuet-Higgins 1997 (§14.3.2) calculated the decay of nonlinear capillary-gravity waves by computing the viscous dissipation of the irrotational flow without vorticity or vorticity layers.

14.2 Viscous decay of capillary waves on drops and bubbles

Now we consider the problem of decay of capillary waves on free surfaces of spherical form. Free-surfaces are gas-liquid surfaces in which the dynamical effects of the gas is neglected. A drop is a liquid sphere with gas outside; a bubble is a gas sphere with liquid outside.

We may consider two types of waves on a spherical surface, capillary waves and gravity waves. Capillary waves are driven by surface tension. Gravity waves are driven by gravity; in the case of spheres some form of central gravity law must be adopted.

In the limit of a large radius of the spherical surface we obtain a plane problem such as the problem of free gravity waves considered in the previous section. The problem of decay of capillary waves or capillary-gravity waves on plane or spherical surfaces can be considered.

In the last section we studied the decay of gravity waves on a plane free surface. The short waves decay monotonically and are well approximated by VPF. The long waves are progressive and the decay of these progressive waves are well approximates by VCVPF. Here we shall show that the same result holds for capillary waves and hence may be expected for capillary-gravity waves.

In the sequel, we shall confine our attention to capillary waves on a spherical surface. The problem of the viscous decay of gravity waves on a globe was considered by Lamb 1932.

The following citation from Lamb §355 makes the point about viscosity and irrotationality in oscillations of a liquid globe. He gives the formula for decay constant τ for $\exp(-t/\tau)$ from the dissipation analysis $\tau = a^2/(n-1)(2n+1)\nu$ and says that

> the most remarkable feature of this result is the excessively minute extent to which the oscillations of a globe of moderate dimensions are affected by such a degree of viscosity as is ordinarily met in nature. For a globe of the size of the earth, and of the same kinematic viscosity as water, we have, on the cgs system, $a = 6.37 \times 10^8$, $\nu = 0.0178$ and the value of τ for the gravitational oscillation of longest period ($n = 2$) is therefore
>
> $$\tau = 1.44 \times 10^{11} \text{ years.}$$